Accepted Manuscript

2,7-naphthyridinone-based MET kinase inhibitors: A promising novel scaffold for antitumor drug development

Lin-Sheng Zhuo, Hong-Chuang Xu, Ming-Shu Wang, Xing-E. Zhao, Zhi-Hui Ming, Xiao-Lei Zhu, Wei Huang, Guang-Fu Yang

PII: S0223-5234(19)30561-6

DOI: https://doi.org/10.1016/j.ejmech.2019.06.033

Reference: EJMECH 11436

To appear in: *European Journal of Medicinal Chemistry*

Received Date: 27 February 2019

Revised Date: 7 June 2019

Accepted Date: 12 June 2019

Please cite this article as: L.-S. Zhuo, H.-C. Xu, M.-S. Wang, X.-E. Zhao, Z.-H. Ming, X.-L. Zhu, W. Huang, G.-F. Yang, 2,7-naphthyridinone-based MET kinase inhibitors: A promising novel scaffold for antitumor drug development, *European Journal of Medicinal Chemistry* (2019), doi: https://doi.org/10.1016/j.ejmech.2019.06.033.

Graphical Abstract

2,7-Naphthyridinone-Based MET Kinase Inhibitors: A Promising Novel Scaffold for Antitumor Drug Development

Lin-Sheng Zhuo[1,†], Hong-Chuang Xu[1,†], Ming-Shu Wang[1,†], Xing-E Zhao[2], Zhi-Hui Ming[2], Xiao-Lei Zhu[1], Wei Huang[1,*], and Guang-Fu Yang[1,*]

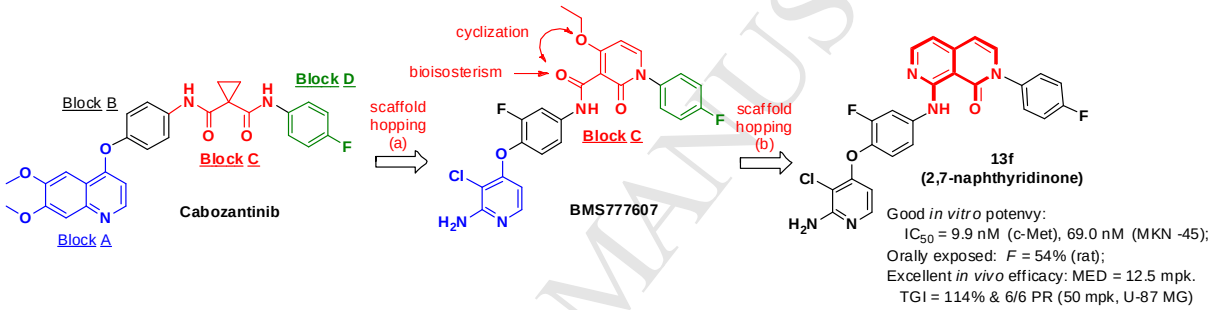

2,7-Naphthyridinone-Based MET Kinase Inhibitors: A Promising Novel Scaffold for Antitumor Drug Development

Lin-Sheng Zhuo[1,†], Hong-Chuang Xu[1,†], Ming-Shu Wang[1,†], Xing-E Zhao[2], Zhi-Hui Ming[2], Xiao-Lei Zhu[1], Wei Huang[1]*, and Guang-Fu Yang[1,]*

[1]*Key Laboratory of Pesticide & Chemical Biology of Ministry of Education, International Joint Research Center for Intelligent Biosensor Technology and Health, College of Chemistry, Central China Normal University, Wuhan 430079, P.R. China*

[2]*Jiangsu Key Laboratory of Molecular Targeted Antitumor Drug Research, Jiangsu Simcere Pharmaceutical Co. Ltd, Nanjing 210042, P. R. China*

** Corresponding authors. E-mail address: weihuangwuhan@126..com (W. Huang), gfyang@mail.ccnu.edu.cn (G. Yang).*

† L.Z.,H.X.and M.W. contributed equally to this work.

ABSTRACT: As part of our effort to develop new molecular targeted antitumor drug, a novel 2,7-naphthyridone-based MET kinase inhibitor, 8-((4-((2-amino-3-chloropyridin-4-yl)oxy)-3-fluorophenyl)amino)-2-(4-fluorophenyl)-2,7-naphthyridin-1(2H)-one (**13f**), was identified. Knowledge of the binding mode of BMS-777607 in MET led to the design of new inhibitors that utilize novel 2,7-naphthyridone scaffold to conformationally restrain the key pharmacophoric groups (block C). Detailed SAR studies resulted in the discovery of a new MET inhibitor **13f**, displaying favorable in vitro potency and oral bioavailability. More importantly, **13f** exhibited excellent in vivo efficacy (tumor growth inhibition/TGI of 114 % and 95 % in 50 mg/kg, respectively) both in the U-87 MG and HT-29 xenograft models. The favorable drug-likeness of **13f** indicated that 2,7-naphthyridinone may be used a promising novel scaffold for antitumor drug development. The preclinical studies of **13f** are under way.

KEYWORDS: 2,7-Naphthyridone, MET kinase inhibitor, Antitumor, In vivo efficacy

1. Introduction

MET is a heterodimeric transmembrane receptor tyrosine kinase (RTK) with a unique structure that is distinct from other RTK families.[1,2] Upon ligand (hepatocyte growth factor, HGF) binding, MET induces several complex signaling pathways resulting in cell proliferation, motility, migration, and survival.[3,4] MET addiction, expedience and inherence have been reported to be associated with cancer onset, progression and therapeutic response.[5,6] Therefore, MET kinase has been considered as an attractive target for molecular targeted therapy in cancers.

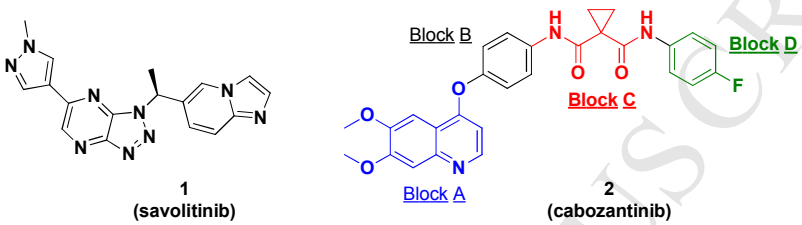

Figure 1. Examples of selective and multi-targeted MET inhibitors

Several MET-targeting agents, including HGF and MET antibodies, as well as small molecule kinase inhibitors, are currently in early or advanced stages of clinical testing.[6-9] Although many structurally diverse small molecule MET kinase inhibitors have been reported, ATP-competitive MET inhibitors can be categorized into two groups based on their chemotypes and binding modes in the MET kinase pocket. Class I inhibitors adopt a U-shape conformation (DFG-in conformation) and interact with the ATP-binding site at the pocket entrance, whereas class II inhibitors bind to MET with a linear conformation (DFG-out conformation) extending from the ATP-binding site to Ile1145 near the C-c-spiral block. Due to their different binding modes, class I and II inhibitors display significantly different characteristics. Compared with class II inhibitors, class I inhibitors have high specificity for MET. For example, Savolitinib (**1**), a selective class I MET inhibitor is in late-stage clinical trial (Figure **1**).[10] Cabozantinib (**2**), a class II inhibitor, the first small molecule multitargeted kinase inhibitor of MET, VEGFR-2 and RET was approved by FDA for the treatment of patients with progressive metastatic medullary thyroid cancer (2012), advanced kidney cancer (2016) and liver cancer who have previously been treated with the medicine sorafenib (2018).[11]

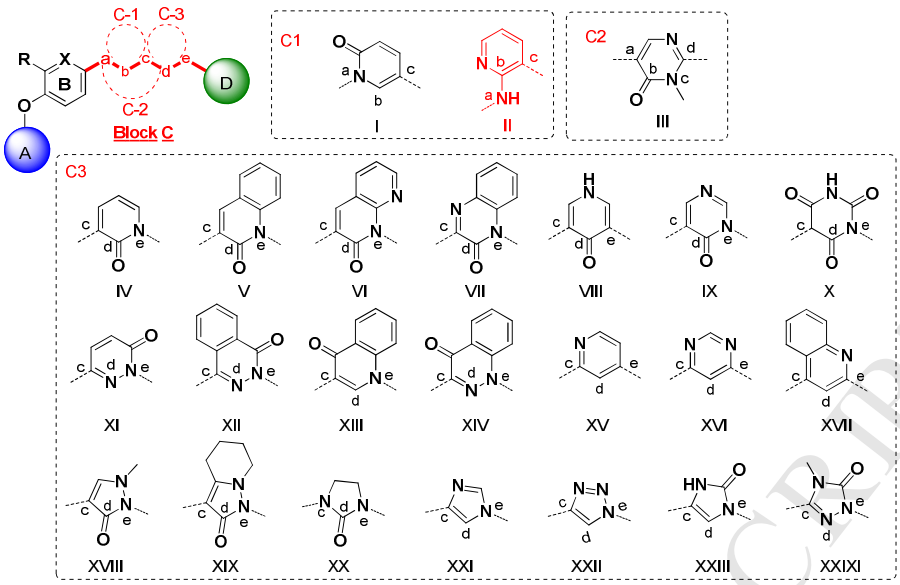

Figure 2. Reported derivatives of Cabozantinib designed by the cyclization strategy of block C

As shown in Figure **1**, The molecular structure of Cabozantinib (**2**) can be divided into four blocks known as A, B, C and D. Among them, the cyclization of block C is the most successful strategy to develop new MET inhibitors (Figure **2**). For example, we reported a new class of pyridine-based class II MET inhibitors with high potency and selectivity by the C-1 cyclization strategy.[18] It's obvious that the key C-3 cyclization strategy resulted in the discovery of many new MET inhibitors bearing pyridone, pyridine, pyrimidinone, pyrimidine, pyridazine, pyrazole, imidazole, triazole cycle and corresponded fused heterocycle, including several clinical candidates, such as BMS-777607 (IV), merestinib (IV), BMS-794833 (VIII), G-773 (IX), RXDX-106 (X), AMG-458 (XVIII) and ningetinib (XVIII).

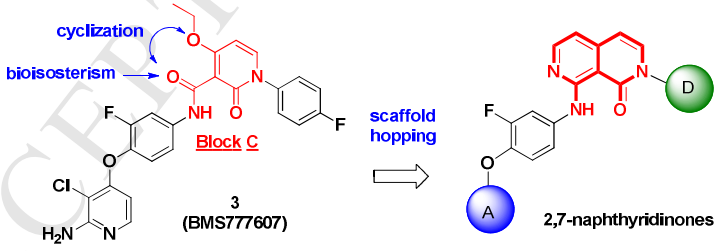

Figure 3. Design of 2,7-naphthyridinone derivatives as new MET inhibitors based on BMS-777606

Compound **3** (BMS-777607), which exhibits desirable drug-likeness and modest selectivity to VEGFR-2, was selected as a starting point for our research.[13] Analysis of the crystal structure of **3** and the MET kinase complex (PDB code, 3F82) revealed that the carbonyl group in pyridone (block C) forms an intramolecular hydrogen-bond (H-bond) with the amide N-H group and a second H-bond with the backbone N-H of Asp1222. The pyridone-based block C assumes a pseudocyclic conformation with maximum deviation from planarity of 0.06 Å in the nitrogen atom of amide group. Herein, we proposed a

scaffold-hopping strategy that utilizes 2,7-naphthyridone to conformationally restrain key pharmacophoric groups within block C of the molecule (Figure **3**). Furthermore, the structure activity relationship (SAR) studies of the block A and block D were carried out to optimize drug-likeness.

2. Chemistry

By the retro-synthetic analysis, the assembly of chlorinated 2,7-naphthyridone **4** (block C-D) with aromatic amine **5** (block A-B) was designed to generate target molecule (Scheme **1**). As diverse aromatic amine **5** could be easily obtained by the reported methods,[19-21] the key point in the synthesis of target compounds was the construction of 8-chloro-2-(4-fluorophenyl)-2,7-naphthyridin-1(2*H*)-one **4**. There were two potential approaches to synthesize **4** according to the cyclization order of the 2,7-naphthyridine ring (Scheme **1**). Method A: pyridinone **6** was first chlorinated to generate tri-substituted pyridine **7**. Naphthyridine **9** was prepared by the condensation of **7** with DMF-DMA, followed by the cyclization of **8** under H_2SO_4. But we failed to introduce the 4-fluorophenyl group into **9** by a common Buchwald cross-coupling reaction. Under the Pd-catalyzed conditions, the dehalogenation was the main reaction, due to the high reactivity of the 8-chlorine atom in naphthyridine, thus making it difficult to obtain **4**.

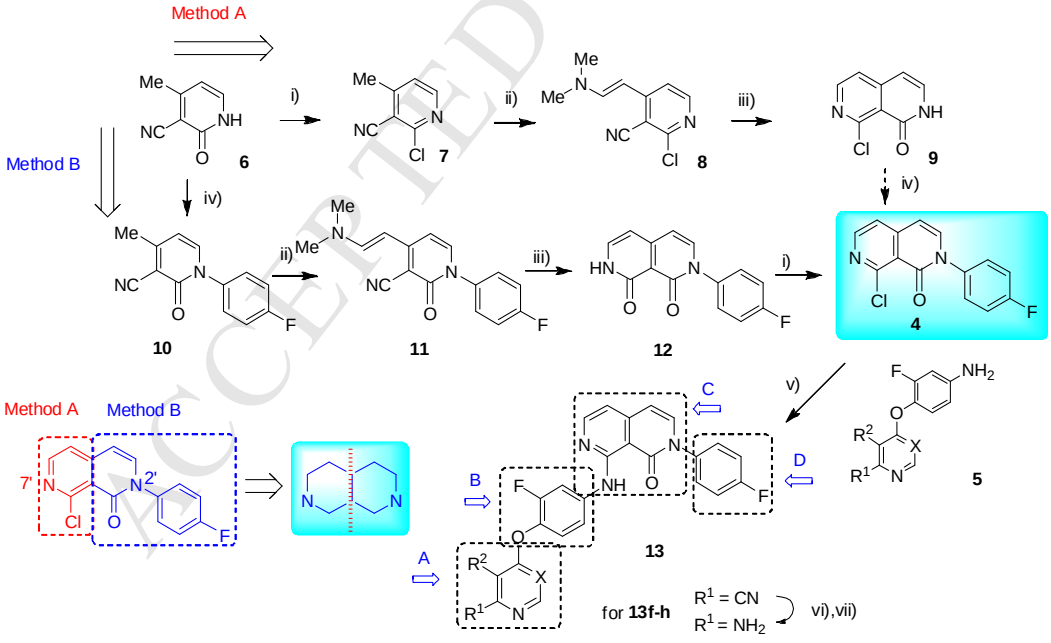

Scheme 1. Reaction conditions and reagents: i) $POCl_3$, 110°C; ii) DMF-DMA, DMF, 90°C; iii) H_2SO_4, 110°C; iv) CuI, DMEDA, K_3PO_4, dioxane, 100°C; v) $Pd_2(dba)_3$, dppp, t-BuONa, dioxane, 100°C; vi) TEMPOH, DCM, 40°C; vii) $PhI(OAc)_2$, ACN, H_2O, 0°C.

After re-analysed the molecular structure of **4**, we found that the nitrogen atoms at 2- and

7-positions were symmetric in the naphthyridine scaffold. Therefore, we modified the synthetic route and developed Method B to construct a chlorinated pyridine unit of 2,7-naphthyridine in the last step. The Ullmann-type coupling of pyridone **6** with 1-fluoro-4-iodobenzene produced the 1-phenyl pyridine-2-one unit of 2,7-naphthyridine (**10**). The condensation of **10** with DMF-DMA followed by H_2SO_4-mediated cyclization and subsequent $POCl_3$-based chlorination successfully yielded the key block C-D intermediate **4**.

With intermediate **4** in hand, compounds **13a-h** were successfully synthesized through direct palladium-catalyzed coupling reactions of **4** and the corresponding aromatic amine **5**. It should be pointed out that, to synthesize **13a-c** bearing a C(2) amino group in the pyridine ring in block A, a cyano group was firstly introduced into the 2- position to improve the coupling reaction. The cyano group was then converted to an amide group with TEMPOH. However, subsequent conventional Hofmann degradation of amide derivatives using typical reagent Br_2-NaOH[22] resulted in a complicated mixture. After optimization, iodo-acetate benzene was eventually identified as an effective reagent with the advantages of good yields, short times, mild conditions and ready isolation of the products.[23]

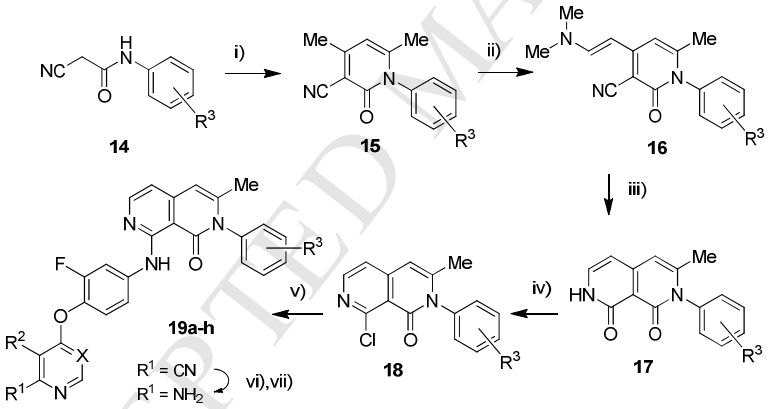

Scheme 2. Reaction conditions and reagents:: i) 2,4-pentanedione, piperidine, EtOH, 90°C; ii) DMF-DMA, DMF, 90°C; iii) H_2SO_4, 110°C; iv) $POCl_3$, 110°C; v) **9**, $Pd_2(dba)_3$, dppp, t-BuONa, dioxane, 100°C; vi) TEMPOH, DCM, 40°C; vii) $PhI(OAc)_2$, ACN, H_2O, 0°C.

As shown in Scheme **2**, the one-step condensation of 2-cyano-N-phenylacetamide **14** with 2,4-pentanedione produced the key pyridine-2-one intermediate **15** in which the N(1) phenyl group in block D was successfully introduced. Similar to the synthesis of **13**, compound **19** was ultimately produced by a condensation-cyclization-chlorination-coupling reaction of **15**. The abolishment of the copper-catalyzed Ullmann-type coupling reaction in the introduction of block D greatly improved the synthetic convenience of **19**.

In addition, the crystal structure of **13f** was determined by X-ray diffraction analysis.[24] In the crystal structure, the block C of **13f** shows good co-planarity, with a max deviation from

planarity of 0.05 Å at N(1) atom. The plane of the 2,7-naphthyridinone and phenyl ring of block B were nearly parallel, with a dihedral angle of 3.5°.

3. Results and discussion

Table 1. Activity of **13a-h** and **19a-h** against MET and VEGFR-2[a]

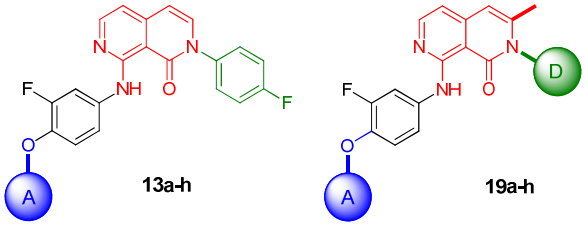

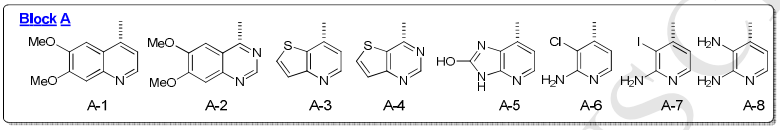

Compd.	Block A	Block D	IC_{50}, nM		
			MET		VEGFR-2
			enzyme-based[a]	cell-based[b]	enzyme-based[a]
13a	A-1	4-F-Ph-	132.5	-[c]	-
13b	A-2	4-F-Ph-	664.2	-	-
13c	A-3	4-F-Ph-	151.9	-	-
13d	A-4	4-F-Ph-	418.8	-	-
13e	A-5	4-F-Ph-	192.0	-	-
13f	A-6	4-F-Ph-	9.9	69.0	279.9
13g	A-7	4-F-Ph-	10.7	116.7	63.2
13h	A-8	4-F-Ph-	103.0	-	-
19a	A-6	4-F-Ph-	1.5	89.8	261.1
19b	A-7	4-F-Ph-	2.4	117.8	102.6
19c	A-6	Ph-	18.0	-	23.1
19d	A-6	2,4-di-F-Ph-	30.5	-	147.9
19e	A-6	4-Cl-Ph-	33.2	-	44.9
19f	A-6	4-CF_3O-Ph-	>1000	-	-
19g	A-7	Ph-	5.5	-	450.7
19h	A-7	2,4-di-F-Ph-	12.6	-	17.3
	3		7.6	46.6	138.7

[a] In vitro kinase assays were performed with the indicated purified recombinant MET or VEGFR-2 kinase domains (nM); [b] IC_{50} values (nM) for HGF-mediated autophosphoylation in MKN-45 cells; [c] Not tested.

The initial SAR study of block A was performed (Table **1**). Compound **13a** bearing the same block A (6,7-dimethoxyquinolin-4-yl) with **2** (Cabozantinib) only displayed moderate

MET inhibitory activity (IC_{50} of 132.5 nM, 17.4-fold lower potency compared with **3**). The replacement of the quinoline with quinazoline (**13b**), thieno[3,2-*b*]pyridine (**13c**), thieno[3,2-*d*]pyrimidine (**13d**), and imidazo[4,5-*b*]pyridin (**13e**), also resulted in a significant loss of potency (IC_{50} of 151.9 nM to 664.2 nM, 20-fold to 87.4-fold lower potency compared with **3**). Interestingly, compound **13f** bearing the same block A (2-amino-3-chloro-pyridin-4-yl) with **3** displayed comparable MET inhibitory activity (IC_{50} of 9.9 nM) to that of compound **3**. The replacement of the 3-chlorine atom with iodine atom provided equivalent potency (**13g**, IC_{50} of 10.7 nM), while the 3-amine-substituted analog **13h** was less potent (IC_{50} of 103.0 nM).

More importantly, **13f** and **13g** displayed comparable cell-based MET inhibitory activity (IC_{50} of 69 nM and 116.7 nM) and VEGFR-2 enzymatic inhibitory activity (IC_{50} of 279.9 nM and 63.2 nM) to that of compound **3** (IC_{50} of 46.6 nM and 138.7 nM). These results indicated that our proposed scaffold hopping strategy was effective to provide novel MET inhibitor.

Subsequently, a methyl group was introduced onto the C(3) position of 2,7-naphthyridine in lead compound **13f**. The resulting compound **19a** (IC_{50} of 1.5 nM) exhibited a 6.6-fold increase in potency compared with **13f** and a 5.1-fold increase relative to **3**. Compound **19b**, bearing 2-amino-3-iodo-pyridin-4-yl group in block A, also displayed excellent inhibitory activity (IC_{50} of 2.4 nM). Meanwhile, **19a** and **19b** also exhibited comparable cell-based MET inhibitory activity (IC_{50} of 89.8 nM and 117.8 nM) and VEGFR-2 enzymatic inhibitory activity (IC_{50} of 261.1 nM and 102.6 nM) to that of compound **3**.

Further SAR validation of block D indicated that the replacement of 4-F atom with 4-H (**19c**, **19g**), 2,4-di-F (**19d**, **19h**) and 4-Cl (**19e**) resulted in the obvious reduction of MET activity (IC_{50} of 18.0 nM and 33.2 nM, 3.7-fold to 22.1-fold less potent) compared with **19a**, while **19f** (4-OCF_3-phenyl group in block D) displayed no inhibitor activity in 1000 nM (Table 1). Moreover, compounds **19c**, **19e** and **19h** showed more potent VEGFR-2 inhibitory activity (IC_{50} of 17.3 nM to 44.9 nM) to that of compound **3**.

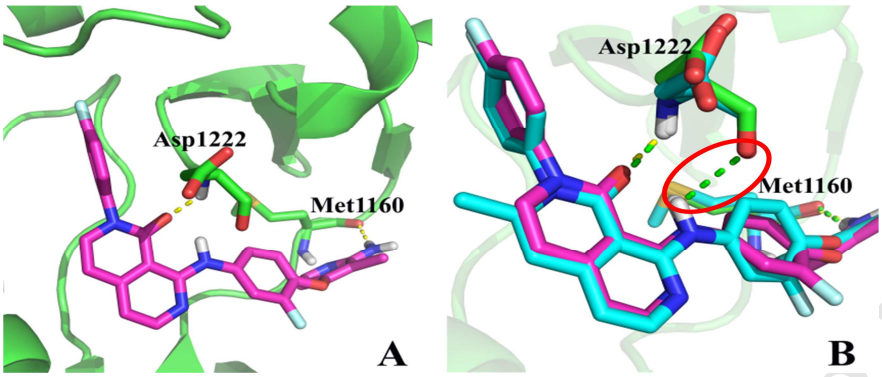

Figure 4. (**A**)The proposed binding mode of **13f** with MET; (**B**) The binding mode overlay of **13f** (magenta) and **19a** (cyan) with MET. The yellow and green dashed lines represent H-bonds between residues with **13f** and **19a**.

Molecular docking was further performed to understand the SAR of block C. As shown in Figure **4A**, the entire molecule of **13f** was favorably located in the MET pocket as expected. Due to the conservation of the key H-bond interactions between the carbonyl group in block C with residues Asp1222, and the amino group in block A with the Met1160, **13f** displayed comparable MET enzymatic activity to that of **3**. The introduction of a C(3) methyl group in block C resulted in a conformational change-induced improvement of the H-bond interactions between **19a** and MET. As shown in Figure **4B**, block C in **19a** assumed an approximately 20° transition compared to **13f**, which led to an additional H-bond between the C(8) N-H group of 2,7-naphthyridine and the side-chain of the Asp1222 residue. As a result, **19a** showed 6.6-fold improved potency over **13f**.

Table 2. Preliminary results of kinase profile of **13f**

kinase	Inhibitory rate (% in 1 μM)	kinase	Inhibitory rate (% in 1 μM)
Aurora-B	44	Lck	75
Axl	97	Lyn	43
DDR2	98	Mer	100
DYRK2	-9	PKA	43
EphA3	38	Ret	96
EphB4	10	Ron	100
Fes	10	Ros	87
Fgr	62	Rse	83
Flt1	95	Src(1-530)	35
Flt4	100	TrkA	99
Fms	88	TrkB	100

The inhibitory activity of compound **13f** against a panel of twenty two other kinases was also assayed (Table **2**). In contrast to its high potency against MET (IC_{50} = 9.9 nM), **13f** also exhibited high inhibitory effects against Axl, DDR2, Flt1, Flt4, Mer, Ret, Ron, TrkA and TrkB (inhibitory rate > 90% in 1 μM). As expected, these data suggested that compound **13f** is a promising multitarget kinase inhibitor. More importantly, it provided a novel scaffold for further selectivity enhancement.

Table 3. In Vivo PK Profiles of Selected Compounds in Rat[a,b]

Compd.	route	Dose (mg/kg)	C_{max} (μg/mL)	T_{max}	$T_{1/2}$	$AUC_{0-\infty}$ (μg* h /mL)	CL (L/h/kg)	*Vz* (L/kg)	*F* (%)
13f	p.o.	10	1.6	1.2	5.1	6.7	-	-	54
	i.v.	2.5	-	-	3.2	3.1	0.8	3.6	-
19a	p.o.	10	3.7	2.3	11.0	21.2	-	-	-
	i.v.	2.5	-	-	7.0	10.5	6.2	2.4	51
19b	p.o.	10	2.7	1.5	4.9	25.7	-	-	-
	i.v.	2.5	-	-	4.2	13.1	0.4	2.9	49

[a] Vehicle: 70% PEG400-30% water. C_{max}, maximum concentration; T_{max}, time of maximum concentration; $T_{1/2}$, half-lif; $AUC_{0-\infty}$, area under the plasma concentration time curve; CL, clearance; V_Z, volume of distribution; *F*, oral bioavailability. [b] Data reported as the average of six animals.

Three potent lead compounds **13f**, **19a** and **19b** were selected for further evaluation of PK properties in rats. As summarized in Table **3**, compound **13f** displayed favorable overall PK profiles, with maximal plasma concentration (C_{max} = 1.6 μg/mL), plasma exposure ($AUC_{0-\infty}$ = 6.7 μg·h/m), and oral bioavailability (*F* = 54%) after oral dose of 10 mg/kg . When the C(3) methyl group was introduced into the 2,7-naphthyridine ring of block, the resulted

compounds **19a** and **19b** exhibited higher C_{max} (3.7 and 2.7 μg/mL) and $AUC_{0-\infty}$ (21.2 and 25.7μg·h/mL), and comparable oral bioavailability (*F* of 51% and 49%) at the same dose.

Table 4. Plasma Protein Binding Data of Compound **13f** in Rat, Mouse and Human (2 μM)

Compd.	Free Fraction %		
	Rat	Mouse	Hunan
13f	< 0.5	< 0.5	< 0.5

The plasma protein binding data of compound **13f** in three different species is listed in Table **4**. As the buffer side response of **13f** is lower than five thousandths of the dose, the plasma protein binding law of **13f** is greater than 99.5%. As far as we know, significant plasma protein binding is common for highly lipophilic compounds.

Table 5. In vivo Tumor Growth Inhibition Activity

Compd.	Tumor model	Dose [a] (mg/kg)	TGI (%)[b]	PR[c]
13f	U-87 MG	12.5	53*	0/6
		25	100**	3/6
		50	114**	6/6
	HT-29	25	50**	0/6
		50	95**	0/6
19a	U-87 MG	25	44	0/6
		40	72	0/6
3	U-87 MG	25	98**	2/6
	HT-29	25	15	0/6

[a] 1Q.D.×21/70% PEG-400/H_2O/p.o.; [b] TGI, Tumor growth inhibition value; *: P<0.05, **: P<0.01; [c] PR, partial regression.

The in vivo antitumor efficacy of **13f** and **19a** were further evaluated in the U-87 MG human glioblastoma xenograft model[20] (Table **5** & Figure **5A**). When administered orally Q.D., two compounds **13f**, **19a** both induced dose-dependent tumor growth inhibition, with the minimum effective doses (MED/ED_{50}, 50% inhibition of tumor growth) of ~12.5, ~32.5 mg/kg, respectively. After dose at 25 mg/kg, **13f** displayed a comparable in vivo efficacy (Tumor Growth Inhibition/TGI of 100%) to that of compound **3** (TGI of 98%). Partial tumor regressions of all animals (PR 6/6, TGI of 114%) were observed at higher doses of **13f** (50 mg/kg).

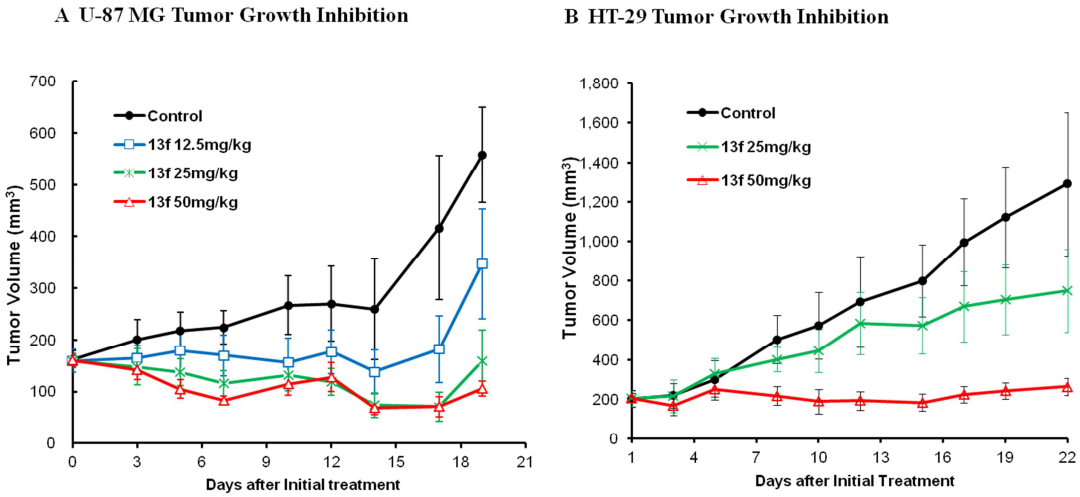

Figure 5. Antitumor efficacy of **13f** in the U-87 MG (**A**) and HT-29 (**B**) xenograft models. Tumor-bearing nude mice were randomly divided into groups when the tumor volume reached 100-200 mm^3 and given **13f** p.o. at the indicated dose levels or vehicle alone over the designated treatment schedule. Data are presented as the mean (± SEM; n = 6 mice per group).

Compound **13f** were further evaluated in the HT-29 human colorectal adenocarcinoma xenograft model (Table **5** & Figure **5B**). In the HT-29 model, **13f** displayed better in vivo efficacy to that of **3** (TGI of 50 *Vs* 15 % inhibition at 25 mg/kg). Moreover, a significant inhibitory effect (TGI of 95%) on tumor growth was observed at a higher dose (50 mg/kg). Taken together, **13f** displayed excellent in vivo efficacy both in the U-87 MG and HT-29 models.

4. Conclusions

In the present work, we described the design, synthesis, and biological evaluation of a series of conformationally constrained 2,7-naphthyridone-based derivatives of BMS-777607 as new MET inhibitors. Extensive SAR studies led to the identification of **13f**, which displayed comparable MET inhibitory activity (IC_{50} = 9.9 nM and 69 nM) to that of BMS-777607 (IC_{50} = 7.6 nM and 46.6 nM) at both the enzyme-based and cell-based assay. More importantly, **13f** exhibited favorable oral bioavailability (54% in rat) and significant in vivo efficacy (TGI of 114 % and 95 % in 50 mg/kg, respectively) both in the U-87 MG and HT-29 xenograft models. The favorable drug-likeness of **13f** indicated that 2,7-naphthyridinone may be used a promising novel scaffold for antitumor drug development. Nowadays, **13f** has been advanced into preclinical studies.

5. Experimental

5.1. General methods

Unless otherwise noted, all chemical reagents were commercially available and treated with standard methods. Silica gel column chromatography (CC). silica gel (200-400 Mesh; Qingdao Makall Group Co., Ltd; Qingdao; China). Solvents were dried in a routine way and redistilled. All reactions involving air- or moisture-sensitive reagents were performed under a nitrogen or argon atmosphere. Melting points of compounds were measured on a Melt-Temp II apparatus and uncorrected. ^{1}H NMR spectra (400 MHz) and ^{13}C NMR (100 MHz) spectra were recorded on a Bruker BioSpin AG (Ultrashield Plus AV 400) spectrometer as deuterochloroform ($CDCl_3$) or dimethyl sulfoxide-d_6 (DMSO-d_6) solutions using tetramethylsilane (TMS) as an internal standard (δ = 0) unless noted otherwise. MS spectra were obtained on an Agilent technologies 6120 quadrupole LC/MS (ESI). High-resolution mass spectra (HR-MS) were obtained on an Agilent 6224 TOF LC/MS (USA) All reactions were monitored using thin-layer chromatography (TLC) on silica gel plates. Yields were of purified compounds and were not optimized.

5.2. General procedures for the synthesis of intermediates

5.2.1 1-(4-fluorophenyl)-4-methyl-2-oxo-1,2-dihydropyridine-3-carbonitrile **(10).**

A dried flask was charged with N,N'-dimethyl-1,2-ethanediamine (14.0 mmol), K_3PO_4 (14.0mmol), 4-methyl-2-oxo-1,2-dihydropyridine-3-carbonitrile **6** (12.7 mmol), CuI (14.0 mmol) and anhydrous dioxane (50 mL) under nitrogen. The mixture was heated to 100 °C and stirred for 12 h, then cooled to room temperature and filtered. The filtrate was concentrated under reduced pressure, and purified by chromatography (CH_2Cl_2/MeOH = 100:1) to yield **10** as a yellow solid (41%). ^{1}H-NMR (400 M, $CDCl_3$) δ 7.44 (d, J = 7.2 Hz, 1H), 7.33-7.36 (m, 2H), 7.17-7.21 (m, 2H), 6.24 (d, J = 7.2 Hz, 1H), 2.51 (s, 3H). MS (ESI). 228.1 $(M)^+$.

5.2.2 (*E*)-4-(2-(dimethylamino)vinyl)-1-(4-fluorophenyl)-2-oxo-1,2-dihydropyridine-3-Carbonitrile **(11).**

A dried flask was charged with N,N-dimethylformamide dimethyl acetal (10 mmol), **10** (10 mmol), and anhydrous DMF (50 mL) under nitrogen. The mixture was heated to 90 °C and stirred for 2 h. The resulted solution was concentrated under reduced pressure, and

purified by chromatography (CH_2Cl_2/MeOH = 50:1) to yield **11** as a yellow solid (93%). ^{1}H-NMR (400 M, $CDCl_3$) δ 7.28-7.35 (m, 3H), 7.11-7.16 (m, 3H), 6.23 (d, J = 7.6 Hz, 1H), 5.42 (d, J = 13.2 Hz, 1H), 2.51 (s, 3H). MS (ESI). 283.1 $(M)^+$.

5.2.3 2-(4-fluorophenyl)-2,7-naphthyridine-1,8(*2H*,*7H*)-dione **(12).**

A solution of **11** (3 mmol) in H_2SO_4 (15 mL) was heated to 110 °C under nitrogen for 2 h. Ice-cold water was added, and the mixture was extracted with dichloromethane. The organic layer was dried and concentrated. The residue was purified by chromatography (CH_2Cl_2/MeOH = 10:1) to yield **12** as a yellow solid (78%). ^{1}H-NMR (400 M, DMSO-*d6*) δ 11.39 (bs, 1H), 7.69 (d, J = 7.2 Hz, 1H), 7.31-7.48 (m, 5H), 6.31-6.40 (m, 2H). MS (ESI). 256.1 $(M)^+$.

5.2.4 8-chloro-2-(4-fluorophenyl)-2,7-naphthyridin-1(*2H*)-one **(4).**

A solution of **12** (2 mmol) in $POCl_3$ (25 mL) was heated to 110 °C under nitrogen for 1 h. Ice-cold water was added, and the mixture was extracted with dichloromethane. The organic layer was dried and concentrated. The residue was purified by chromatography (CH_2Cl_2/MeOH = 50:1) to yield **4** as a yellow solid (85%). ^{1}H-NMR (400 M, $CDCl_3$) δ 8.50 (d, J = 4.2 Hz, 1H), 7.77 (d, J = 7.2 Hz, 1H), 7.67 (d, J = 4.2 Hz, 1H), 7.52-7.56 (m, 2H), 7.37-7.41 (m, 2H), 6.73 (d, J = 7.2 Hz, 1H). MS (ESI). 274.0 $(M)^+$.

5.2.5 1-(4-fluorophenyl)-4,6-dimethyl-2-oxo-1,2-dihydropyridine-3-carbonitrile **(15a).**

A solution of **14** (5 mmol), pentane-2,4-dione (5 mmol) and piperidine in EtOH (50 mL) was heated to 90 °C under nitrogen for 2 h, then cooled to room temperature and filtered. The filtrate was concentrated under reduced pressure to yield **15a** as a white solid (90%). ^{1}H-NMR (400 M, $CDCl_3$) δ 7.16-7.26 (m, 4H), 6.14 (s, 1H), 2.45 (s, 3H), 2.03 (s, 3H). MS (ESI). 242.0 $(M)^+$.

5.2.6 (*E*)-4-(2-(dimethylamino)vinyl)-1-(4-fluorophenyl)-6-methyl-2-oxo-1,2-dihydro-pyridine-3-carbonitrile **(16a).**

Prepared according to the procedure for the preparation of **11**, from **15a**, to yield **16a** as yellow solid (75%). ^{1}H-NMR (400 M, $CDCl_3$) δ 7.16-7.30 (m, 5H), 6.12 (s, 1H), 5.37 (d, J = 13.2 Hz, 1H), 2.95 (s, 6H), 1.93 (s, 3H). MS (ESI). 297.1 $(M)^+$.

5.2.7 2-(4-fluorophenyl)-3-methyl-2,7-naphthyridine-1,8(2*H*,7*H*)-dione **(17a).**

Prepared according to the procedure for the preparation of **12**, from **16a**, to yield **17a** as

yellow solid (80%). ^{1}H-NMR (400 M, DMSO-*d6*) δ 11.23 (bs, 1H), 7.34-7.43 (m, 5H), 6.32 (s, 1H), 6.18 (bs, 1H), 1.90 (s, 3H). MS (ESI). 270.0 $(M)^+$.

5.2.8 8-chloro-2-(4-fluorophenyl)-3-methyl-2,7-naphthyridin-1(2*H*)-one **(18a).**

Prepared according to the procedure for the preparation of **4**, from **17a**, to yield **18a** as yellow solid (84%). ^{1}H-NMR (400 M, $CDCl_3$) δ 8.39 (d, J = 5.6 Hz, 1H), 7.20-7.31 (m, 4H), 6.36 (s, 1H), 2.08 (s, 3H). MS (ESI). 288.0 $(M)^+$.

5.2.9 8-chloro-3-methyl-2-phenyl-2,7-naphthyridin-1(2*H*)-one **(18b).**

Prepared according to the procedure for the preparation of **18a**, from 2-cyano-*N*-phenylacetamide (**14b**), to yield **18b** as yellow solid. ^{1}H-NMR (400 M, $CDCl_3$) δ 8.39 (d, J = 5.2 Hz, 1H), 7.46-7.56 (m, 3H), 7.20-7.28 (m, 3H), 6.34 (s, 1H), 2.03 (s, 3H). MS (ESI). 270.0 $(M)^+$.

5.2.10 8-chloro-2-(2,4-difluorophenyl)-3-methyl-2,7-naphthyridin-1(2*H*)-one **(18c).**

Prepared according to the procedure for the preparation of **18a**, from 2-cyano-*N*-(2,4-difluorophenyl)acetamide (**14c**), to yield **18c** as yellow solid. ^{1}H-NMR (400 M, $CDCl_3$) δ 8.41 (d, J = 5.6 Hz, 1H), 7.21-7.29 (m, 3H), 7.02-7.08 (m, 3H), 6.39 (s, 1H), 2.07 (s, 3H). MS (ESI). 306.0 $(M)^+$.

5.2.11 8-chloro-2-(4-chlorophenyl)-3-methyl-2,7-naphthyridin-1(2*H*)-one **(18d).**

Prepared according to the procedure for the preparation of **18a**, from *N*-(4-chlorophenyl)-2-cyanoacetamide (**14d**), to yield **18d** as yellow solid. ^{1}H-NMR (400 M, $CDCl_3$) δ 8.40 (d, J = 5.2 Hz, 1H), 7.52 (d, J = 8.8 Hz, 1H), 7.17-7.26 (m, 3H), 6.37 (s, 1H), 2.04 (s, 3H). MS (ESI). 304.0 $(M)^+$.

5.2.12 8-chloro-3-methyl-2-(4-(trifluoromethoxy)phenyl)-2,7-naphthyridin-1(2*H*)-one **(18e).**

Prepared according to the procedure for the preparation of **18a**, from 2-cyano-*N*-(4-(trifluoromethyl)phenyl)acetamide (**14e**), to yield **18e** as yellow solid. ^{1}H-NMR (400 M, $CDCl_3$) δ 8.41 (d, J = 5.2 Hz, 1H), 7.21-7.38 (m, 5H), 6.37 (s, 1H), 2.05 (s, 3H). MS (ESI). 354.0 $(M)^+$.

5.3. General procedures for the synthesis of targets 13a-13h and 19a-19h

5.3.1 8-((4-((6,7-dimethoxyquinolin-4-yl)oxy)-3-fluorophenyl)amino)-2-(4-fluorophenyl)-2,7-naphthyridin-1(2*H*)-one **(13a)**.

A dried flask was charged with **4** (1 mmol), 1,3-Bis(diphenylphosphino)propane (20 mmol %), sodium tert-butoxide (1.2 mmol), $Pd_2(dba)_3$ (10 mmol %), 4-((6,7-dimethoxy-quinolin-4-yl)oxy)-3-fluoroaniline **5a** and anhydrous dioxane (15 mL) under nitrogen. The mixture was heated to 100 °C and stirred for 3 h, then cooled to room temperature and filtered. The filtrate was concentrated under reduced pressure, and purified by chromatography (CH_2Cl_2 /MeOH = 20:1) to yield 8-((4-((6,7-dimethoxyquinolin-4-yl)oxy) -3-fluorophenyl)amino)-2-(4-fluorophenyl)-2,7-naphthyridin-1(2*H*)-one **13a** as a yellow solid (55%). M.p. 255-256 °C. ^{1}H-NMR (400 M, $CDCl_3$) δ 12.11 (s, 1H), 8.37-8.40 (m, 2H), 7.83 (s, 1H), 7.52 (d, J = 6.8 Hz, 1H), 7.46 (d, J = 6.4 Hz, 1H), 7.39-7.42 (m, 2H), 7.30-7.33 (m, 2H), 7.24-7.28 (m, 2H), 6.87 (d, J = 4.4 Hz, 1H), 6.53 (d, J = 6.4 Hz, 1H), 6.34-6.37 (m, 2H), 4.00 (s, 3H) , 3.73 (s, 3H); ^{13}C-NMR (100 M, $CDCl_3$) δ 177.3, 164.1, 163.3, 156.2, 155.6, 155.1, 153.4, 150.5, 147.3, 145.9, 142.0, 138.2, 136.2, 129.1, 128.6, 122.1, 121.0, 116.9, 116.7, 111.8, 110.8, 109.5, 108.4, 107.6, 106.2, 105.8, 98.2, 56.3, 56.0. MS (ESI). 553.0 $[M+H]^+$. HR-MS (EI) m/z calcd for $C_{31}H_{22}F_2N_4O_4$, 552.1609; found 552.1638 $[M]^+$.

5.3.2 8-((4-((6,7-dimethoxyquinazolin-4-yl)oxy)-3-fluorophenyl)amino)-2-(4-fluoro-phenyl)-2,7-naphthyridin-1(2*H*)-one (**13b)**.

Prepared according to the procedure for the preparation of **13a**, from 4-((6,7-dimethoxyquinazolin-4-yl)oxy)-3-fluoroaniline **5b** and **4**, to yield **13b** as yellow solid (61%), M.p. 199-200 °C. ^{1}H-NMR (400 M, $CDCl_3$) δ 11.86 (s, 1H), 8.64 (s, 1H), 8.34 (d, J = 4.4 Hz, 1H), 8.25 (d, J = 6.4 Hz, 1H), 7.59 (s, 1H), 7.40-7.46 (m, 4H), 7.23-7.29 (m, 4H), 6.76 (d, J = 4.4 Hz, 1H), 6.48 (d, J = 6.4 Hz, 1H), 4.08 (s, 6H); ^{13}C-NMR (100 M, DMSO-d_6) δ 182.1, 165.0, 163.3, 157.1, 156.6, 155.1, 153.8, 150.9, 150.2, 149.0, 146.5, 138.3, 136.1, 130.5, 130.0, 128.9, 125.1, 117.2, 116.8, 110.8, 109.1, 108.7, 107.9, 106.7, 105.8, 100.8, 56.6. MS (ESI). 553.9 $[M+H]^+$. HR-MS (EI) m/z calcd for $C_{30}H_{21}F_2N_5O_4$, 553.1562; found 554.1640 $[M+H]^+$.

5.3.3 8-((3-fluoro-4-(thieno[3,2-*b*]pyridin-7-yloxy)phenyl)amino)-2-(4-fluorophenyl)-2,7-naphthyridin-1(*2H*)-one **(13c).**

Prepared according to the procedure for the preparation of **13a**, from 3-fluoro-4-(thieno[3,2-*b*]pyridin-7-yloxy)aniline **5c** and **4**, to yield **13c** as yellow solid

(50%), M.p. 125-126 °C. ^{1}H-NMR (400 M, $CDCl_3$) δ 11.93 (s, 1H), 8.58 (d, J = 5.6 Hz, 1H), 8.38-8.34 (m, 3H),7.43-7.21 (m, 7H), 7.09 (t, J = 9.2 Hz, 1H), 6.81 (d, J = 5.4Hz, 1H), 6.52 (d, J =5.6 Hz, 1H), 6.49 (d, J =5.4 Hz, 1H); ^{13}C-NMR (100 M, $CDCl_3$) δ 163.1, 162.9, 161.2, 160.4, 158.8, 156.3, 155.6, 150.6, 150.1, 145.8, 139.2, 136.3, 136.0, 130.7, 128.7, 125.2, 123.4, 122.0, 116.8, 116.6, 116.4, 110.3, 109.4, 106.5, 106.1, 103.1. MS (ESI). 498.8 $[M+H]^+$. HR-MS (EI) m/z calcd for $C_{27}H_{16}F_2N_4O_2S$, 498.0962; found 499.1045 $[M+H]^+$.

5.3.4 8-((3-fluoro-4-(thieno[3,2-*d*]pyrimidin-4-yloxy)phenyl)amino)-2-(4-fluorophenyl)-2,7-naphthyridin-1(*2H*)-one **(13d).**

Prepared according to the procedure for the preparation of **13a**, from 3-fluoro-4-(thieno[3,2-*d*]pyrimidin-4-yloxy)aniline **5d** and **4**, to yield **13d** as yellow solid (66%), M.p. 155-156°C. ^{1}H-NMR (400 M, $CDCl_3$) δ 11.86 (s, 1H), 8.72 (s, 1H), 8.34 (d, J = 5.4 Hz, 1H), 8.23 (d, J =10.5 Hz, 1H), 7.97 (d, J = 5.4Hz, 1H), 7.50 (d, J = 5.5Hz, 1H), 7.42-7.21 (m, 7H), 6.77 (d, J = 5.4Hz, 1H), 6.48 (d, J =7.4 Hz, 1H); ^{13}C-NMR (100 M, $CDCl_3$) δ 163.2, 161.2, 160.4, 156.3, 155.4, 154.4, 152.3, 150.7, 145.8, 139.4, 139.3, 136.4, 135.9, 135.2, 133.7, 128.7, 123.4, 117.3, 116.8, 116.6, 116.1, 110.1, 109.1, 108.9, 106.5, 106.1. MS (ESI). 499.8 $[M+H]^+$. HR-MS (EI) m/z calcd for $C_{26}H_{15}F_2N_5O_2S$, 499.0915; found 500.1002 $[M+H]^+$.

5.3.5 8-((3-fluoro-4-((2-hydroxy-3H-imidazo[4,5-*b*]pyridin-7-yl)oxy)phenyl)amino)-2-(4-fluorophenyl)-2,7-naphthyridin-1(*2H*)-one **(13e).**

Prepared according to the procedure for the preparation of **13a**, from 7-(4-amino-2-fluorophenoxy)-3H-imidazo[4,5-b]pyridin-2-ol **5e** and **4**, to yield **13e** as yellow solid (62%),, M.p. 222-223 °C. ^{1}H-NMR (400 M, DMSO-*d6*) δ 11.98 (s, 1H), 11.37 (s, 1H), 11.23 (s, 1H), 8.35 (d, J = 5.4 Hz, 1H), 8.29 (d, J = 11.2 Hz, 1H), 7.76 (d, J = 6.0 Hz, 1H), 7.71 (d, J = 7.3 Hz, 1H), 7.60-7.57 (m, 2H), 7.47-7.39 (m, 3H), 7.30 (t, J = 9.0 Hz, 1H), 7.03 (d, J = 5.4Hz, 1H), 6.71 (d, J = 7.3 Hz, 1H), 6.33 (d, J =6.0 Hz, 1H); ^{13}C-NMR (100 M, DMSO-*d6*) δ 162.8, 162.6, 160.2, 155.4, 154.5, 154.2, 150.0, 146.8, 145.7, 141.4, 138.5, 138.4, 137.8, 136.6, 129.5, 123.1, 116.2, 115.9, 112.1, 110.8, 108.3, 105.8, 105.2, 104.0. MS (ESI). 499.1 $[M+H]^+$; HR-MS (EI) m/z calcd for $C_{26}H_{16}F_2N_6O_3$, 498.1252; found 521.1141 $[M+Na]^+$.

5.3.6 8-((4-((2-amino-3-chloropyridin-4-yl)oxy)-3-fluorophenyl)amino)-2-(4-fluorophenyl)-2,7-naphthyridin-1(*2H*)-one **(13f).**

A dried flask was charged with **4** (1 mmol), 1,3-Bis(diphenylphosphino)propane (20 mmol %), sodium tert-butoxide (1.2 mmol), $Pd_2(dba)_3$ (10 mmol %), 4-(4-amino-2-fluorophenoxy)-3-chloropicolinonitrile **5f** and anhydrous dioxane (15 mL) under nitrogen. The mixture was heated to 100 °C and stirred for 3 h, then cooled to room temperature and filtered. The filtrate was concentrated under reduced pressure, and purified by chromatography (CH_2Cl_2/MeOH = 20:1) to yield 3-chloro-4-(2-fluoro-4-((7-(4-fluoro phenyl)-8-oxo-7,8-dihydro-2,7-naphthyridin-1-yl)amino)phenoxy)picolinonitrile as a yellow solid (80%). A solution of above nitrile derivative (1 mmol) and 2,2,6,6-tetramethyl piperidin-1-ol (5 mmol) in CH_2Cl_2 (10 mL)was heated to 40 °C for 5 h. The resulted solution was concentrated under reduced pressure, and purified by chromatography (CH_2Cl_2/MeOH =30:1) to yield 3-chloro-4-(2-fluoro-4-((7-(4-fluoro-phenyl)-8-oxo-7,8-dihydro-2,7-naphthyridin-1-yl)amino)phenoxy)picolinamide as a yellow solid (63%). A solution of above carboxy amide derivative (1 mmol) and (diacetoxyiodo)benzene (1.1 mmol) in acetonitrile (10 mL) was stired at 0 °C for 1 h. The resulted solution was concentrated under reduced pressure, and purified by chromatography (CH_2Cl_2/MeOH = 20:1) to yield **13f** as a yellow solid (78%), M.p. 244-245 °C. ^{1}H-NMR (400 M, DMSO-*d6*) δ 11.83 (s, 1H), 8.34 (d, *J* = 4.4 Hz, 1H), 8.18 (d, *J* = 8.0 Hz, 1H), 7.78 (bs, 1H), 7.37-7.41 (m, 2H), 7.35 (d, *J* = 8.0 Hz, 1H), 7.23-7.28 (m, 4H), 7.09 (t, *J* = 7.2 Hz, 1H), 6.77 (d, *J* = 4.4 Hz, 1H), 6.48 (d, *J* = 4.8 Hz, 1H), 5.04 (s, 2H); ^{13}C-NMR (100 M, $CDCl_3$) δ 164.0, 163.2, 162.5, 162.0, 156.5, 156.0, 155.3, 152.9, 150.6, 146.7, 145.8, 139.0, 136.3, 135.4, 128.7, 123.1, 116.9, 115.3, 110.2, 109.1, 106.5, 106.0, 102.4. MS (ESI). 491.8 $[M+H]^+$. HR-MS (EI) m/z calcd for $C_{30}H_{26}FN_5O_2$, 491.0961; found 492.1029 $[M+H]^+$.

5.3.7 8-((4-((2-amino-3-iodopyridin-4-yl)oxy)-3-fluorophenyl)amino)-2-(4-fluorophenyl)-2,7-naphthyridin-1(*2H*)-one **(13g).**

Prepared according to the procedure for the preparation of **13f**, from 4-(4-amino-2-fluorophenoxy)-3-iodopicolinonitrile **5g** and **4**, to yield **13g** as yellow solid (33%), M.p. 251-252 °C. ^{1}H-NMR (400 M, DMSO-*d6*) δ 11.91 (s, 1H), 8.47 (s, 1H), 8.19 (d, *J* = 11.2 Hz, 1H), 7.90 (d, *J* = 7.6 Hz, 1H), 7.73 (d, *J* = 5.6 Hz, 1H), 7.63-7.59 (m, 2H),

7.45-7.41 (m, 3H), 7.26 (t, *J* = 9.2 Hz, 1H), 6.81 (d, *J* = 7.6 Hz, 1H), 6.22 (s, 2H), 5.80 (d, *J* = 5.6 Hz, 1H); ^{13}C-NMR (100 M, DMSO-*d6*) δ 164.2, 163.0, 162.6, 161.8, 161.3, 154.7, 152.4, 149.7, 148.9, 143.1, 140.1, 138.5, 136.7, 135.9, 129.9, 123.8, 117.0, 116.7, 116.5, 115.3, 109.1, 108.8, 107.0, 101.4, 100.1. MS (ESI). 583.0 $[M]^+$. HR-MS (EI) m/z calcd for $C_{25}H_{16}F_2IN_5O_2$, 583.0317; found 584.0396 $[M+H]^+$.

5.3.8 8-((4-((2,3-diaminopyridin-4-yl)oxy)-3-fluorophenyl)amino)-2-(4-fluorophenyl)-2,7-naphthyridin-1(*2H*)-one **(13h).**

Prepared according to the procedure for the preparation of **13f**, from 3-amino-4-(4-amino-2-fluorophenoxy)picolinonitrile **5h** and **4**, to yield **13h** as yellow solid (36%), M.p. 230-231 °C. ^{1}H-NMR (400 M, DMSO-*d6*) δ 11.91 (s, 1H), 8.33 (d, *J* = 5.4 Hz, 1H), 8.23 (d, *J* = 11.2 Hz, 1H), 7.71 (d, *J* = 7.4 Hz, 1H), 7.61-7.56 (m, 2H), 7.43-7.37 (m, 3H), 7.21 (d, *J* = 5.7 Hz, 1H), 7.10 (t, *J* = 9.1 Hz, 1H), 7.01 (d, *J* = 5.4 Hz, 1H), 6.70 (d, *J* = 7.4 Hz, 1H), 5.90 (d, *J* = 5.6 Hz, 1H), 5.55 (s, 2H), 4.48 (s, 2H) ; ^{13}C-NMR (100 M, DMSO-*d6*) δ 162.5, 160.3, 155.4, 154.3, 151.9, 150.2, 149.9, 148.1, 145.7, 137.6, 137.2, 136.5, 136.3, 135.6, 129.4, 122.2, 118.3, 116.1, 116.0, 115.8, 110.4, 108.1, 105.6, 105.1, 101.5. MS (ESI). 473.1 $[M+H]^+$. HR-MS (EI) m/z calcd for $C_{25}H_{18}F_2N_6O_2$, 472.1459; found 473.1541 $[M+H]^+$.

5.3.9 8-((4-((2-amino-3-chloropyridin-4-yl)oxy)-3-fluorophenyl)amino)-2-(4-fluoro-phenyl)-3-methyl-2,7-naphthyridin-1(*2H*)-one **(19a).**

Prepared according to the procedure for the preparation of **13f**, from 8-chloro-2-(4-fluorophenyl)-3-methyl-2,7-naphthyridin-1(2*H*)-one **18a** and **5f**, to yield **19a** as yellow solid (35%), M.p. 213-214 °C. ^{1}H-NMR (400 M, DMSO-d_6) δ 11.90 (s, 1H), 8.25-8.30 (m, 2H), 7.74 (d, *J* = 4.4 Hz, 1H), 7.47-7.50 (m, 3H), 7.40-7.43 (m, 2H),7.26 (t, *J* = 7.2 Hz, 1H), 6.91 (d, *J* = 4.4 Hz, 1H), 6.65 (s, 1H), 6.35 (s, 2H), 5.92 (d, *J* = 4.4 Hz, 1H), 1.99 (s, 3H); ^{13}C-NMR (100 M, $CDCl_3$) δ 163.7, 163.1, 160.6, 159.9, 157.4, 155.2, 154.4, 152.0, 149.7, 145.5, 145.2, 134.4, 134.2, 130.8, 123.3, 116.5, 116.0, 110.1, 108.1, 106.5, 104.8, 104.4, 100.1, 21.2. MS (ESI). 506.1 $[M+H]^+$. HR-MS (EI) m/z calcd for $C_{26}H_{18}ClF_2N_5O_2$, 505.1117; found 506.1184 $[M+H]^+$.

5.3.10 8-((4-((2-amino-3-iodopyridin-4-yl)oxy)-3-fluorophenyl)amino)-2-(4-fluorophenyl)-3-methyl-2,7-naphthyridin-1(*2H*)-one **(19b).**

Prepared according to the procedure for the preparation of **13f**, from 8-chloro-2-(4-fluorophenyl)-3-methyl-2,7-naphthyridin-1(2*H*)-one **18a** and **5g**, to yield **19b** as yellow solid (35%), M.p. 223-224 °C. ^{1}H-NMR (400 M, DMSO-d_6) δ 11.90 (s, 1H), 8.30 (d, J = 5.5 Hz, 1H), 8.26 (d, J = 11.2 Hz, 1H), 7.73 (d, J = 5.6 Hz, 1H), 7.50-7.40 (m, 5H), 7.22 (t, J = 9.1 Hz, 1H), 6.91 (d, J = 5.5 Hz, 1H), 6.65 (s, 1H), 6.16 (s, 2H), 5.80 (d, J = 5.5 Hz, 1H), 1.99 (s, 3H); ^{13}C-NMR (100 M, DMSO-d_6) δ 164.1, 163.7, 160.9, 160.1, 157.6, 155.3, 154.5, 149.8, 149.3, 145.5, 145.3, 134.5, 134.3, 130.8, 130.7, 123.3, 116.5, 116.3, 116.0, 110.0, 108.2, 106.5, 104.8, 104.4, 100.2, 21.3. MS (ESI). 598.0 $[M+H]^+$. HR-MS (EI) m/z calcd for $C_{26}H_{18}F_2IN_5O_2$, 597.0473; found 598.0561 $[M+H]^+$.

5.3.11 8-((4-((2-amino-3-chloropyridin-4-yl)oxy)-3-fluorophenyl)amino)-3-methyl-2-phenyl-2,7-naphthyridin-1(*2H*)-one **(19c).**

Prepared according to the procedure for the preparation of **13f**, from 8-chloro-3-methyl-2-phenyl-2,7-naphthyridin-1(2*H*)-one **18b** and **5f**, to yield **19c** as yellow solid (62%), M.p. 201-202 °C. ^{1}H-NMR (600 M, $CDCl_3$) δ 11.78 (s, 1H), 8.28 (d, J = 5.4 Hz, 1H), 8.18 (d, J = 12.0 Hz, J_2=3.6 Hz, 1H), 7.77 (d, J = 6.0 Hz, 1H), 7.61-7.27 (m, 4H), 7.06 (t, J = 9.1 Hz, 1H), 6.70 (t, J = 4.8 Hz, 1H), 6.37 (s, 1H), 6.07 (d, J = 6.0 Hz, 1H), 5.31 (d, J = 5.4 Hz, 1H), 4.94 (s, 2H), 2.03 (s, 3H); ^{13}C-NMR (100 M, DMSO-d_6) δ 163.6, 159.9, 157.4, 155.2, 154.4, 152.0, 147.2, 145.4, 145.2, 138.9, 138.8, 138.0, 134.4, 134.2, 129.6, 128.8, 128.5, 123.3, 116.0, 110.0, 108.0, 107.8, 104.7, 104.4, 100.0, 21.3. MS (ESI). 488.0 $[M+H]^+$. HR-MS (EI) m/z calcd for $C_{26}H_{19}ClFN_5O_2$, 487.1211; found 487.1285 $[M]^+$.

5.3.12 8-((4-((2-amino-3-chloropyridin-4-yl)oxy)-3-fluorophenyl)amino)-2-(2,4-difluoro-phenyl)-3-methyl-2,7-naphthyridin-1(*2H*)-one **(19d).**

Prepared according to the procedure for the preparation of **13f**, from 8-chloro-2-(2,4-difluorophenyl)-3-methyl-2,7-naphthyridin-1(2*H*)-one **18c** and **5f**, to yield **19d** as yellow solid (47%), M.p. 210-211 °C. ^{1}H-NMR (400 M, DMSO-d_6) δ 11.73 (s, 1H), 8.33 (d, J = 5.2 Hz, 1H), 8.27 (d, J = 11.2 Hz, 1H), 7.75 (d, J = 5.6 Hz, 1H), 7.71-7.27 (m, 4H), 7.30 (t, J = 8.8 Hz, 1H), 6.94 (d, J = 5.2 Hz, 1H), 6.71 (s, 1H), 6.44 (s, 2H), 5.92 (d, J = 5.6 Hz, 1H), 2.03 (s, 3H); ^{13}C-NMR (100 M, DMSO-d_6) δ 161.6, 161.4, 161.3, 161.2, 157.4,157.3,

155.2, 151.0, 121.3, 116.1, 106.1, 106.0, 102.8, 102.2, 22.5. MS (ESI). 524.1[M+H]$^+$. HR-MS (EI) m/z calcd for $C_{26}H_{17}ClF_3N_5O_2$, 523.1023; found 524.1108 [M+H]$^+$.

5.3.13 8-((4-((2-amino-3-chloropyridin-4-yl)oxy)-3-fluorophenyl)amino)-2-(4-chlorophenyl)-3-methyl-2,7-naphthyridin-1(*2H*)-one **(19e).**

Prepared according to the procedure for the preparation of **13f**, from 8-chloro-2-(4-chlorophenyl)-3-methyl-2,7-naphthyridin-1(2*H*)-one **18d** and **5f**, to yield **19e** as yellow solid (57%), M.p. 221-222 °C. ^{1}H-NMR (400 M, $CDCl_3$) δ 11.70 (s, 1H), 8.28 (d, J = 5.2 Hz, 1H), 8.18 (d, J = 10.8 Hz, 1H), 7.77 (d, J = 5.6 Hz, 1H), 7.58-7.20 (m, 5H), 7.07 (t, J = 8.8 Hz, 1H), 6.69 (d, J = 5.2 Hz, 1H), 6.37 (s, 1H), 6.06 (m, 1H), 4.97 (s, 2H), 2.19 (s, 3H); ^{13}C-NMR (100 M, DMSO-d_6) δ 163.6, 159.8, 157.4, 155.2, 154.4, 152.0, 149.8, 147.2, 145.2, 138.8, 138.7, 136.9, 134.4, 134.3, 133.5, 130.6, 129.6, 123.3, 116.0, 110.1, 108.1, 107.8, 104.9, 104.3, 100.0, 21.2. MS (ESI). 522.0 [M+H]$^+$. HR-MS (EI) m/z calcd for $C_{26}H_{18}Cl_2FN_5O_2$, 521.0822; found 522.0891 [M+H]$^+$.

5.3.14 8-((4-((2-amino-3-chloropyridin-4-yl)oxy)-3-fluorophenyl)amino)-3-methyl-2-(4-(trifluoromethoxy)phenyl)-2,7-naphthyridin-1(*2H*)-one **(19f).**

Prepared according to the procedure for the preparation of **13f**, from 8-chloro-3-methyl-2-(4-(trifluoromethoxy)-phenyl)-2,7-naphthyridin-1(2*H*)-one **18e** and **5f**, to yield **19f** as yellow solid (39%), M.p. 233-234 °C. ^{1}H-NMR (400 M, $CDCl_3$) δ 11.67 (s, 1H), 8.29 (d, J = 5.2 Hz, 1H), 8.18 (d, J = 10.8 Hz, 1H), 7.78 (d, J = 5.2 Hz, 1H), 7.43-7.07 (m, 6H), 6.70 (d, J = 5.2 Hz, 1H), 6.38 (d, J = 5.2 Hz, 1H), 6.06 (s, 1H), 4.95 (s, 2H), 2.04 (s, 3H); ^{13}C-NMR (100 M, DMSO-d_6) δ 163.6, 159.8, 157.4, 155.2, 154.4, 152.0, 149.8, 148.2, 147.2, 145.2, 138.8, 137.0, 134.4, 130.8, 123.3, 122.2, 121.3, 118.7, 116.0, 110.2, 108.1, 107.9, 104.9, 104.3, 100.8, 100.0, 21.2. MS (ESI). 572.0 [M+H]$^+$. HR-MS (EI) m/z calcd for $C_{27}H_{18}ClF_4N_5O_3$, 571.1034; found 572.1109 [M+H]$^+$.

5.3.15 8-((4-((2-amino-3-iodopyridin-4-yl)oxy)-3-fluorophenyl)amino)-3-methyl-2-phenyl-2,7-naphthyridin-1(*2H*)-one **(19g).**

Prepared according to the procedure for the preparation of **13f**, from **18b** and **5g**, to yield **19g** as yellow solid (56%), M.p. 218-219 °C. ^{1}H-NMR (400 M, DMSO-d_6) δ 11.96 (s, 1H), 8.30 (d, J = 5.6 Hz, 1H), 8.25 (d, J = 11.2 Hz, 1H), 7.73 (d, J = 5.6 Hz, 1H), 7.62-7.40 (m, 6H), 7.24 (t, J = 9.1 Hz, 1H), 6.92 (d, J = 5.6 Hz, 1H), 6.66 (s, 1H), 6.32 (s, 2H), 5.81

(d, J = 5.6 Hz, 1H), 1.98 (s, 3H); ^{13}C-NMR (100 M, DMSO-d_6) δ 164.6, 163.6, 160.2, 155.2, 154.3, 149.7, 148.0, 145.5, 145.2, 138.9, 138.8, 138.0, 134.5, 129.6, 128.8, 128.5, 123.3, 116.0, 110.1, 108.0, 107.8, 104.7, 104.4, 99.6, 21.3. MS (ESI). 58.0 $[M+H]^+$. HR-MS (EI) m/z calcd for $C_{26}H_{19}FIN_5O_2$, 579.0567; found 580.0643 $[M+H]^+$.

5.3.16 8-((4-((2-amino-3-iodopyridin-4-yl)oxy)-3-fluorophenyl)amino)-2-(2,4-difluorophenyl)-3-methyl-2,7-naphthyridin-1(*2H*)-one **(19h).**

Prepared according to the procedure for the preparation of **13f**, from **18c** and **5g**, to yield **19h** as yellow solid (56%), M.p. 225-226 °C. ^{1}H-NMR (400 M, DMSO-d_6) δ 11.71 (s, 1H), 8.33 (d, J = 5.6 Hz, 1H), 8.26 (d, J = 12.0 Hz, 1H), 7.73 (d, J = 5.6 Hz, 1H), 7.70-7.34 (m, 4H), 7.23 (t, J = 9.2 Hz, 1H), 6.93 (d, J = 5.2 Hz, 1H), 6.71 (s, 1H), 6.20 (s, 2H), 5.78 (d, J = 5.6 Hz, 1H), 2.03 (s, 3H); ^{13}C-NMR (100 M, DMSO-d_6) δ 164.1, 163.2, 160.9, 155.2, 154.4, 151.9, 150.3, 149.3, 145.4, 145.1, 138.5, 135.0, 132.1, 123.3, 121.8, 116.2, 112.7, 112.5, 110.2, 108.3, 108.0, 105.3, 105.0, 103.9, 99.6, 20.6. MS (ESI). 616.0 $[M+H]^+$. HR-MS (EI) m/z calcd for $C_{26}H_{19}FIN_5O_2$, 615.0379; found 616.0468 $[M+H]^+$.

5.4. Molecular docking.

The three dimensional (3D) structure of the MET kinase complex (PDB code: 3F82) and VEGFR-2 kinase (PDB code: 3U6J) complex was obtained from PDB database. All water molecules and ligand were removed from the complex structure and hydrogen atoms were added with pH equaling to 7.0 using Sybyl-X. The AutoDock 4.2[25] program was applied to docking compound **13f** and **19a** into the binding site of MET kinase or VEGFR-2 kinase. The Gasteiger charges were used for these inhibitors. In the docking process, a conformational search was performed for the ligand using the Solis and Wets local search method, and the Lamarckian genetic algorithm (LGA)[26,27] was applied for the conformational search of the binding complex of ligand with two kinases. Among a series of docking parameters, the grid size was set to be 70x70x80 in 3F82, 46x40x60 in 3U6J, and the used grid space was the default value of 0.375 Å. Among a set of 100 candidates of the docked complex structures, the best one was first selected according to the interaction energy and was then compared with the conformation of ligand (**3**, BMS-777607) extracted from the crystal structure.

5.5. In Vivo Antitumor Activity Assay.

Female nude mice (4-6 weeks old) were housed and maintained under specific-pathogen free conditions. Animal experiments were performed according to institutional ethical guidelines of animal care. Tumor cells were inoculated into the flanks of athymic nude mice (2×10^6 cells/mouse). When the tumor volume reached about 100-200 mm^3, the mice were randomly assigned into control and treatment groups. Control groups were given vehicle alone, and treatment groups received synthesized compounds as indicated doses via p.o. administration 7 days per week for 3 weeks. The sizes of the tumors were measured three times per week using microcaliper. The tumour volume (V) was calculated as follows: V =[length (mm) $\times$width^2 (mm^2)]/2. Percent (%) inhibition values (TGI) were measured on the final day of study for drug treated compared with vehicle-treated mice and were calculated as 100% × (1- ((treated$^{\text{final day}}$−treated$^{\text{day 0}}$)/control$^{\text{final day}}$ −control$^{\text{day 0}}$)). Significant differences between the treated versus the control groups ($P \leq 0.01$) were determined using Student's.

Acknowledgement

This work was supported by the National Key Research and Development Program of China (No. 2017YFA0505200), the National Natural Science Foundation of China (No. 201502063), the Natural Science Foundation of Hubei Province (No. 2016CFB562) and the self-determined research funds of CCNU from the colleges' basic research and operation of MOE (No. CCNU18TS009).

Appendix A. Supplementary data

Supplementary data related to this article can be found at.

References

[1] D. P. Bottaro, J. S. Rubin, D. L. Faletto, A. M. Chan, T. E. Kmiecik, G. F. Vande Woude, S. A. Aaronson, Identification of the hepatocyte growth factor receptor as the c-Met proto-oncogene product, Science 251 (1991) 802–804.

[2] L. Naldini, K. M. Weidner, E. Vigna, G. Gaudino, A. Bardelli, C. Ponzetto, R. P. Narsimhan, G. Hartmann, R. Zarnegar, G. K. Michalopoulos, Scatter factor and hepatocyte growth factor are indistinguishable ligands for the MET receptor, EMBO J. 10 (1991) 2867–2678.

[3] L. Trusolino, A. Bertotti, P. M. Comoglio, MET signalling: principles and functions in development, organ regeneration and cancer, Nat. Rev. Mol. Cell Biol. 11 (2010) 834–848.

[4] E. Gherardi, W. Birchmeier, C. Birchmeier, G. Vande Woude, Targeting MET in cancer: rationale and progress, Nat. Rev. Cancer 12 (2012) 89–103.

[5] W. Birchmeier, E. Gherardi, G. F. Vande Woude, Met, metastasis, motility and more, Nat. Rev. Mol. Cell Biol. 4 (2003) 915–925.

[6] P. M. Comoglio, L. Trusolino, C. Boccaccio, Known and novel roles of the MET oncogene in cancer: a coherent approach to targeted therapy, Nat. Rev. Cancer. 18 (2018) 341–358.

[7] J. J. Cui, Targeting receptor tyrosine kinase MET in cancer: small molecule inhibitors and clinical progress, J. Med. Chem. 57 (2014) 4427–4453.

[8] P. C. Lv, Z. C. Wang, H. L. Zhu, Recent Advances in the Design and Synthesis of c-Met Inhibitors as Anticancer Agents (2014-Present), Curr. Med. Chem. 24 (2017) 57–64.

[9] P. K. Parikh, M. D. Ghate, Recent advances in the discovery of small molecule c-Met Kinase inhibitors, Eur. J. Med. Chem. 143 (2018) 1103–1138.

[10] H. Jia, G. Dai, J. Weng, Z. Zhang, Q. Wang, F. Zhou, L. Jiao, Y. Cui, Y. Ren, S. Fan, J. Zhou, W. Qing, Y. Gu, J. Wang, Y. Sai, W. Su, Discovery of (S)-1-(1-(Imidazo[1,2-a]pyridin-6-yl)ethyl)-6-(1-methyl-1H-pyrazol-4-yl)-1H-[1,2,3]triazolo[4,5-b]pyrazine (volitinib) as a highly potent and selective mesenchymal-epithelial transition factor (c-Met) inhibitor in clinical development for treatment of cancer, J. Med. Chem. 57 (2014) 7577–7789.

[11] G. K. Abou-Alfa, A. E. Borgman-Hagey, R. K. Kelley, Cabozantinib in Hepatocellular Carcinoma, N. Engl. J. Med. 379 (2018) 1384–1385.

[12] M. Zillhardt, S. M. Park, I. L. Romero, K. Sawada, A. Montag, T. Krausz, S. D. Yamada, M. E. Peter, E. Lengyel, Foretinib (GSK1363089), an orally available multikinase inhibitor of c-Met and VEGFR-2, blocks proliferation, induces anoikis, and impairs ovarian cancer metastasis, Clin. Cancer Res. 17 (2011) 4042–4051.

[13] G. M. Schroeder, Y. An, Z. W. Cai, X. T. Chen, C. Clark, L. A. Cornelius, J. Dai, J. Gullo-Brown, A. Gupta, B. Henley, J. T. Hunt, R. Jeyaseelan, A. Kamath, K. Kim, J. Lippy, L. J. Lombardo, V. Manne, S. Oppenheimer, J. S. Sack, R. J. Schmidt, G. Shen, K. Stefanski, J. S. Tokarski, G. L. Trainor, B. S. Wautlet, D. Wei, D. K. Williams, Y. Zhang, Y. Zhang, J. Fargnoli, R. M. Borzilleri, Discovery of N-(4-(2-amino-3-chloropyridin-4-yloxy)-3-fluorophenyl)-4-ethoxy-1-4-fluorophenyl)-2-oxo-1,2-dihydro-pyridine-3-carboxamide (BMS-777607), a selective and orally efficacious inhibitor of the Met kinase superfamily, J. Med. Chem. 52 (2009) 1251–1254.

[14] H. Fujita, K. Miyadera, M. Kato, Y. Fujioka, H. Ochiiwa, J. Huang, K. Ito, Y. Aoyagi, T. Takenaka, T. Suzuki, S. Ito, A. Hashimoto, T. Suefuji, K. Egami, H. Kazuno, Y. Suda, K. Nishio, K. Yonekura, The novel VEGF receptor/MET-targeted kinase inhibitor TAS-115 has marked in vivo antitumor properties and a favorable tolerability profile, Mol. Cancer Ther. 12 (2013) 2685–2696.

[15] P. P. Patwardhan, K. S. Ivy, E. Musi, E. de Stanchina, G. K. Schwartz, Significant blockade of

multiple receptor tyrosine kinases by MGCD516 (Sitravatinib), a novel small molecule inhibitor, shows potent anti-tumor activity in preclinical models of sarcoma, Oncotarget. 7 (2016) 4093–4109.

[16] Q. Tang, Y. Zhao, X. Du, L. Chong, P. Gong, Design, synthesis, and structure activity relationships of novel 6, 7-disubstituted-4-phenoxyquinoline derivatives as potential antitumor agents, Eur. J. Med. Chem. 69 (2013) 77–89.

[17] S. Li, Q. Huang, Y.J. Liu, X.L. Zhang, S. Liu, C. He, P. Gong, Design, synthesis and antitumour activity of bisquinoline derivatives connected by 4-oxy-3-fluoroaniline moiety, Eur. J. Med. Chem. 64 (2013) 62–73.

[18] N. F. She, L. S. Zhuo, W. Jiang, X. L. Zhu, J. Wang, Z. H. Ming, X. E. Zhao, X. Cong, W. Huang, Design, Synthesis and Evaluation of Highly Selective Pyridone-based Class II MET Inhibitors, Bioorg. Med. Chem. Lett. 24 (2014) 3351–3355.

[19] O. M. Saavedra, S. W. Claridge, L. Zhan, F. Raeppel, A. Vaisburg, S. Raeppel, R. Deziel, M. Mannion, N. Z. Zhou, L. Isakovic, Thienopyridine and thienopyrimidine derivatives and their preparation, pharmaceutical compositions, and use as inhibitors of VEGF receptor and HGF receptor signaling for treatment of proliferative diseases, WO2005030140A2, 2004-09-24.

[20] M. Mannion, S. Raeppel, S. Claridge, N. Zhou, O. Saavedra, L. Isakovic, L. Zhan, F. Gaudette, F. Raeppel, R. Déziel, N. Beaulieu, H. Nguyen, I. Chute, C. Beaulieu, I. Dupont, M. F. Robert, S. Lefebvre, M. Dubay, J. Rahil, J. Wang, H. Ste-Croix, M. A. Robert, J. M. Besterman, A. Vaisburg, N-(4-(6,7-Disubstituted-quinolin-4-yloxy)-3-fluorophenyl)-2-oxo-3-phenyl-imidazolidine-1-carboxa mides: a novel series of dual c-Met/VEGFR2 receptor tyrosine kinase inhibitors, Bioorg. Med. Chem. Lett. 19 (2009) 6552–6556.

[21] L. C. Bannen, D. S. Chan, J. Chen, L. E. Dalrymple, T. P. Forsyth, T. P. Huynh, V. Jammalamadaka, R. G. Khoury, J. W. Leahy, M. B. Mac, G. Mann, L. W. Mann, J. M. Nuss, J. Parks, C. S. Takeuchi, Y. Wang, W. Xu, Preparation of quinolines and quinazolines as inhibitors of c-Met and other tyrosine kinases and therapeutic uses against proliferative diseases, WO2007054831A2, 2006-05-19.

[22] H. Togo, T. Nabana, K. Yamaguchi, Preparation and reactivities of novel (diacetoxyiodo)arenes bearing heteroaromatics, J. Org. Chem. 65 (2000) 8391–8394.

[23] A. M. Palmer, G. Munch, C. Scheufler, W. Kromer, Synthesis and pharmacological evaluation of 5-carboxmide-substituted tetrahydrochromeno[7,8-d]imidazoles, Tet. Lett. 50 (2009) 3920–3922.

[24] Full crystallographic details has been deposited at the Cambridge Crystallographic Data Center and allocated the deposition number CCDC 1899394 (**13f**).

[25] G. M. Morris, R. Huey, W. Lindstrom, M. F. Sanner, R. K. Belew, D. S. Goodsell, A. J. Olson, Autodock4 and AutoDockTools4: automated docking with selective receptor flexibility, J. Comput Chem. 30 (2009) 2785–2791.

[26] G. M. Morris, D. S. Goodsell, R. S. Halliday, R. Huey, W. E. Hart, R. K. Belew, A. J. Olson, Automated docking using a lamarckian genetic algorithm and an empirical binding free energy function, J. Comput. Chem. 19 (1998) 1639–1662.

[27] D. Sitkoff, K. A. Sharp, B. Honig, Accurate calculation of hydration free energies using macroscopic solvent models. J. Phys Chem. 98 (1994) 1978–1988.

Highlights:

2,7-Naphthyridinone-Based MET Kinase Inhibitors: A Promising Novel Scaffold for Antitumor Drug Development

- 2,7-Naphthyridinone was developed as a promising scaffold for the discovery of new MET-targeted antitumor drug.
- The 2,7-naphthyridone fragment was utilized to conformationally restrain key pharmacophoric groups (block C) of BMS-777607 and resulted in the discovery of a new potent MET inhibitor **13f**.
- Favorable in vitro potency, pharmacokinetic profiles and in vivo antitumor efficacy make **13f** a promising drug candidate to advance into preclinical development.